

## RESEARCH ARTICLE

# Characterization of Wild-Type and Mutated *RET* Proto-Oncogene Associated with Familial Medullary Thyroid Cancer

Mohammad Hosein Masbi<sup>1</sup>, Javad Mohammadiasl<sup>2</sup>, Hamid Galehdari<sup>3</sup>, Ahmad Ahmadzadeh<sup>4</sup>, Mohammad Amin Tabatabaiefar<sup>2</sup>, Neda Golchin<sup>1</sup>, Vahid Haghpanah<sup>5</sup>, Fakher Rahim<sup>6\*</sup>

## Abstract

**Background:** We aimed to assess *RET* proto-oncogene polymorphisms in three different Iranian families with medullary thyroid cancer (MTC), and performed molecular dynamics simulations and free energy stability analysis of these mutations. **Materials and Methods:** This study consisted of 48 patients and their first-degree relatives with MTC confirmed by pathologic diagnosis and surgery. We performed molecular dynamics simulations and free energy stability analysis of mutations, and docking evaluation of known *RET* proto-oncogene inhibitors, including ZD-6474 and ponatinib, with wild-type and mutant forms. **Results:** The first family consisted of 27 people from four generations, in which nine had the C.G2901A (P.C634Y) mutation; the second family consisted of six people, of whom three had the C.G2901T (P.C634F) mutation, and the third family, who included 12 individuals from three generations, three having the C.G2251A (P.G691S) mutation. The automated 3D structure of *RET* protein was predicted using I-TASSER, and validated by various protein model verification programs that showed more than 96.3% of the residues in favored and allowed regions. The predicted instability indices of the mutated structures were greater than 40, which reveals that mutated *RET* protein is less thermo-stable compared to the wild-type form (35.4). **Conclusions:** Simultaneous study of the cancer mutations using both in silico and medical genetic procedures, as well as onco-protein inhibitor binding considering mutation-induced drug resistance, may help in better overcoming chemotherapy resistance and designing innovative drugs.

**Keywords:** Hereditary MTC - mutation - *RET* proto-oncogene - in silico - inhibitor binding

*Asian Pac J Cancer Prev*, 15 (5), 2027-2033

## Introduction

Thyroid cancer is the most predominant neoplasm of endocrine system and is responsible for around 1% of human malignancies (Nikiforova et al., 2008). Medullary thyroid carcinoma (MTC) is account for 5-10% of all thyroid malignancies, which is originated from the parafollicular C cells of the thyroid (Othman et al., 2009; Matias-Guiu et al., 2013).

MTC may occur sporadically or as part of the inherited cancer syndrome multiple endocrine neoplasia type 2 (MEN 2), which is classified into three clinically distinct subtypes: MEN 2A, MEN 2B, and familial MTC (FMTC) (Kouvaraki et al., 2005). MEN 2 syndromes are inherited as an autosomal dominant condition and therefore, 50% of the patient's first-degree relatives are at risk of carrying the mutated gene.

Patients with MEN 2A develop MTC, primary hyperparathyroidism (PHP), and pheochromocytoma (PHEO), hence MEN 2B patients are at risk for MTC, PHEO, mucosal neuromas, ganglioneuromas of the digestive tract, or skeletal abnormalities (Punales et al., 2004). In almost all cases, activation of the *RET* proto-oncogene is known as the cause of the MEN 2 syndromes. The germline mutations in MEN 2A syndromes have been described in *RET* proto-oncogene exons 5, 8, 10, 11, 13, 14, and 15 (Kouvaraki et al., 2005). Mutations in MEN 2A syndromes exclusively affect cysteine residues in the extracellular domain (Mulligan et al., 1995), which create an unpaired residue and finally result in constitutive activation of the signaling pathway (Santoro et al., 2004). However, most of the MEN 2A cases have mutations of one of the conserved cysteine residues at codons 609, 611, 618 and 620 in exon 10 and codon 634 in exon 11 in the

<sup>1</sup>Noor Genetic Diagnostic Laboratory, <sup>2</sup>Department of Medical Genetics, Faculty of Medicine, <sup>3</sup>Health Research Institute, Hearing Research Center, <sup>4</sup>Health Research Institute, Thalassemia and Hemoglobinopathies Research Center, Ahvaz Jundishapur University of Medical Sciences, <sup>5</sup>Faculty of Science, Genetic Department, Shahid Chamran University, Ahvaz, <sup>6</sup>Endocrinology and Metabolism Research Center, Endocrinology and Metabolism Clinical Sciences Institute, Endocrinology and Metabolism Research Institute, Tehran University of Medical Sciences Tehran, Iran \*For correspondence: Bioinfo2003@ajums.ac.ir

extracellular domain of *RET* (Eng et al., 1996).

We observed the *RET* proto-oncogene polymorphism in three different Iranian families with MTC, and performed molecular dynamics (MD) simulations and free energy stability analysis of these mutations. However, we have also performed MD simulations, docking and binding free energy evaluations of the known *RET* proto-oncogene inhibitors binding with the wild-type and mutants form.

## Materials and Methods

### Study design and population

This prospective study consisted of 48 patients and their first-degree relatives with the MTC evidence confirmed by pathologic diagnosis and surgery. This research was approved by the Ahvaz Jundishapur University of Medical Sciences Ethical Committee. All participants gave written informed consent to take part in the study under the Declaration of Helsinki.

### DNA preparation, PCR and sequencing

Following the approval of the local ethics committee of Ahvaz Jundishapur University of Medical Sciences, peripheral blood samples were obtained. Genomic DNA was isolated from peripheral blood of the patients, their parents and several normal individuals using the QIAamp DNA Mini Kit (QIAGEN Inc., Valencia, CA, USA) based on the manufacturer's instruction. All coding exons of hot spot *RET* proto-oncogene and the flanking intronic regions were amplified by polymerase chain reaction (PCR). Then all PCR fragments were sequenced using designed primers, containing *RET* exon 10, the following primers were used: (10F 5'GCGCCCCAGGAGGCTGATGC3') and (10R 5'CGTGGTGGTCCCGGCCGCC3'). The *RET* exon 11 was amplified using following primers: (11AF 5'CCTCTGCGGTGCCAAGCCTC3') and (11AR 5'CACCGGAAGAGGAGTAGCTG3') (Hedayati et al, 2006).

The reaction mixture (30 $\mu$ l) contain 2 $\mu$ l of genomic DNA, 1 $\mu$ l of each upstream and downstream primer (diluted to 10 $\mu$ mol/L), 11 $\mu$ l of ddH<sub>2</sub>O, 15 $\mu$ l of 2 $\times$ Taq PCR Master Mix (Qiagen Inc.) were used. PCR were implemented as denaturation at 95°C for 3min, followed by 40 thermal cycles composed of 94°C for 30 sec, at 55°C for 30 sec, and at 72°C for 45 sec for each. Besides, the amplified products were isolated by electrophoresis on a 1% agarose gel and then purified using the QIAamp purification kit (Qiagen Inc.), and the nucleotide sequence was determined by direct sequencing using an ABI 310 automatic sequencer according to the manufacturer's instructions (Applied Biosystem, Foster City, CA, USA).

### Modeling of wild-type and mutant *RET*

Proteins: Wild-type human *RET* protein sequence was *RETR*ieved from UNIPROT (entry: P07949). Homology modeling of the wild-type and mutated proteins were generated by MODELLER 9 (Sali et al., 1993). Hence, the predicted models by MODELLER were of poor quality with inappropriate folded conformation as a good quality model, they could not be obtained even by using multiple templates. Moreover, we modeled *RET* protein segment

which consists of 1114 amino acid residues by I-TASSER server (Zhang, 2008). For the submitted sequences, five 3D models were obtained and considering the lowest energy the best model was selected. Furthermore, the mutant structures were made as a point mutations in native proteins at C.G2901T (P.C634F) (cysteine to phenylalanine), C.G2901A (P.C634Y) (cysteine to tyrosine) and C.G2251A (p.G691S) (glycine to serine) using SPDB viewer (Kaplan et al., 2001). The wild-type and mutant structures were energetically optimized by applying the all atom OPLS force field available under the GROMACS 4.5 package (Pronk et al., 2013). The quality of wild-type and mutated model structures was verified using the PROCHECK (Laskowski et al., 1996), Verify 3D (Bowie et al., 1991), ERRAT (Colovos et al., 1993), and PROSA (Wiederstein et al., 2007) programs. The physiochemical properties of wild-type and mutated proteins were computed using ExPasy ProtParam tools.

### Mutant and wild-type docking experiments

The modeled structures were cleaned; water and ions removed, structures energy was minimized, and flexibility set for side chains and protonation of nonpolar residues using AutoDock Tools (Cosconati et al., 2010). The structure of ligand molecules vandetanib (ZD-6474:DB05294), a novel targeted therapy for the treatment of metastatic or locally advanced medullary thyroid cancer (Ton et al., 2013), and ponatinib (AP24534: DB08901), a novel potent inhibitor of oncogenic *RET* mutants associated with thyroid cancer (De Falco et al., 2013), was *RETR*ieved from PubChem, Drug Bank and the energy minimized in PDB files using Marvin Draw program, with the flexibility and protonation status set. Docking was performed with 1000 conformations of the *RET* wild-type and mutants, and the results were analyzed and rendered in PyMOL. The final dock energy and estimated free energy charge of binding were calculated using the following formulas: *Estimated free energy charge of binding* ( $\Delta G$ )=*final intermolecular energy+torsional free energy of ligand*

### Free energy simulations

Calculations of the *RET* protein stabilities, binding free energy using AMBER force field (Wang et al., 2004), and the solvation energy term based on the continuum generalized Born and solvent-accessible surface area (GB/SA) solvation model (Srinivasan et al., 1998; Kollman et al., 2000), were done. The MM-GBSA model typically was used in free energy simulations according to the previous studies (Verkhivker et al., 2002; 2003).

### Protein stability calculations

The destabilization effects of the selected *RET* mutations and the protein stability change upon these mutations were computed. For this purpose three different tools were used, including CUPSAT (Parthiban et al., 2006), FOLDx (Schymkowitz et al., 2005), MM-GBSA free energy calculations (Kollman et al., 2000), Mupro (Cheng et al., 2006), and SDM, a server for predicting effects of mutations on protein stability and malfunction (Worth et al., 2011).

## Results

### Initial genetic analysis

We have analyzed the coding region of *RET* proto-oncogene in 45 Iranian patients with MTC from three different families. We observed three mutations previously reported, which were present in heterozygosity in exon 11, including C.G2901T (P.C634F), C.G2901A (P.C634Y), and G961S. Family one consisted of 27 people from four generations, in which 9 have the C.G2901A (P.C634Y) mutation (Figure 1). The second family has an obviously negative family history for relevant thyroid disorders and hypertension. The study included six individuals from two generations. We observed one mutation previously reported, which were present in heterozygosity in exon 11, in family consisted of six people, in which three have the C.G2901T (P.C634F) mutation (Figure 2). Third family included 12 individuals from three generations. From the second generation two people have the history of MTC, but the mutation was not observed because they were not alive in time of observation. We observed one mutation previously reported, which were present in heterozygosity in exon 11, in family consisted of 12 people, in which five have the C.G2251A (P.G691S) mutation (Figure 3).

### Homology modeling of the *RET* and model validation

Though, the 3D structures of *RET* protein have not been reported in RCSB PDB Data bank, the available models (PDBID: IXPD, residues 1-340, and PDBID: 2IVS, residues 713-1112) have not included our mutations sites (residues 634 and 691). Then, 3D model of *RET* protein (UNIPROT entry: P07949) was predicted by homology modeling using MODELLER 9.10 with multiple templates. The obtained 3D models were of poor quality with inappropriate folded conformations. Therefore, the automated 3D structure of *RET* protein was predicted based on the sequence-to-structure-to-function model using I-TASSER (Figure 4A). Using different protein model verifications programs showed

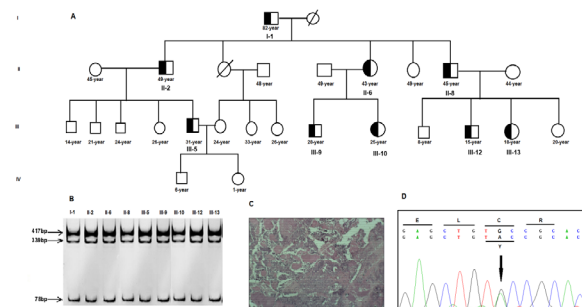


**Figure 1. A) Pedigree of the MTC family carrying a C.G2901A (P.C634Y) RET Mutation; B) Portion of DNA Sequences and Polyacrylamide Gel Electrophoresis Analysis of Restriction Endonuclease Digestion Showing Paternal Origin MEN 2A (I-1, II-2, II-6, II-8, III-5, III-12 and III-13) and Maternal Origin (III-9 and III-10) were Heterozygous for C.G2901A (P.C634Y); C) Biopsy of The Thyroid Mass Showing Around to Polygonal Tumor Cells with Vesicular Nuclei; D) Sanger Traces Showing a Heterozygous G>A changes**

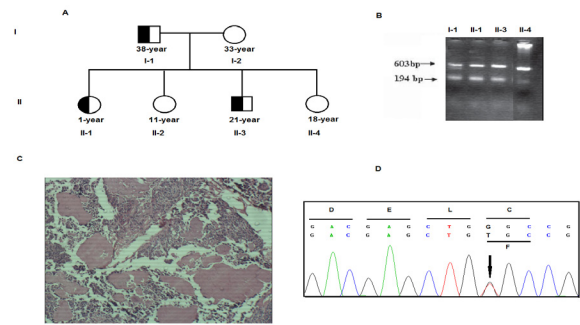


**Figure 2. A) Pedigree of the MTC Family Carrying a C.G2901T (P.C634F) RET Mutation; B) Portion of DNA Sequences and Polyacrylamide Gel Electrophoresis Analysis of Restriction Endonuclease Digestion Showing Paternal Origin MEN 2A (I-1, II-2, and II-3) were Heterozygous for C.G2901T (P.C634F); Biopsy of the Thyroid Mass Showing Around to Polygonal Tumor Cells with Vesicular Nuclei; D) Sanger Traces Showing a Heterozygous G>T Changes**

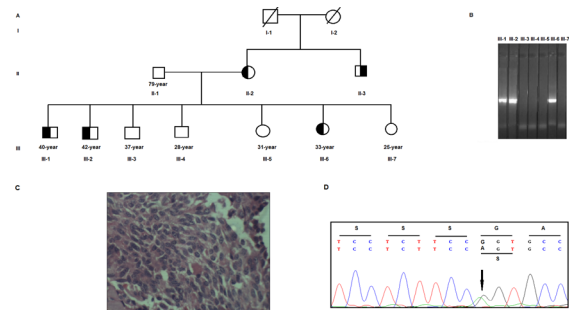


**Figure 3. A) Pedigree of the MTC Family Carrying a C.G2251A (P.G691S) RET Mutation; B) Portion of DNA Sequences and Polyacrylamide Gel Electrophoresis Analysis of Restriction Endonuclease Digestion Showing Maternal Origin MEN 2A (II-2, II-3, III-1, III-2, and III-6) were Heterozygous for C.G2251A (P.G691S); Biopsy of the Thyroid Mass Showing Around to Polygonal Tumor Cells with Vesicular Nuclei; D) Sanger Traces Showing a Heterozygous G>A Changes**

more than 96.3% of the residues were found to be in favored and allowed regions, which validate the quality of homology model (Figure 4B). The overall G-factor for selected model was found to be -0.39 which is greater than the acceptable value -0.50, and therefore suggested that modeled structure is acceptable. The modeled structure was also validated by Verify 3D which assigned 51.57% had averaged 3D-1D score has >0.2 for the modeled protein. The secondary structure of target protein *RET* has mixed secondary structures, including alpha-helices, beta-strands and coils (Figure 4C). ERRAT2 shows 95.6% overall quality factors indicating good resolution structure. However, quality of the model were compared to reference structure of high resolution obtained from X-Ray crystallography analysis through Z score, which was -6.51 showing the possibility to be a better model.

The physiochemical properties of wild-type and mutated proteins were computed and the data presented. The computed isoelectric point (pI) value of protein

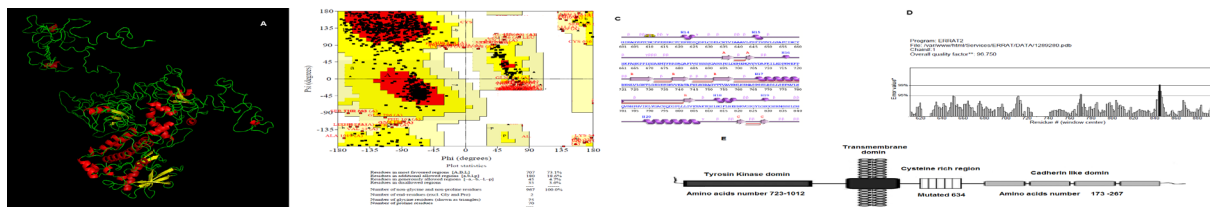


**Figure 4. A) The Best Predicted Model: Helix, Beta Sheets and Turns are in Red, Yellow and Green Color, Respectively Modeled by I-TASSER Program; B) Ramachandran Plot of Modeled Structure Validated by PROCHECK Program (96.3% of the Residues were Found to be in Favored and Allowed Regions); C) The Secondary Structure of Target Protein RET has mixed Secondary Structures, Including Alpha-Helices, Beta-Strands and Coils; D) ERRAT Result Also has Been Given; E) Schematic Diagram Depicting *RET* Onco-Protein Domains and the Location of the Mutations of Interest**

determined as 6.17 ( $pI < 7$ , revealing the acidic nature of the wild-type and mutated *RET* proteins). The predicted Instability index of the mutated structures were greater than 40, which reveals that mutated *RET* protein is less thermo-stable compared to the wild-type form (Instability index of a protein smaller than 40 makes it stable while more than 40 considered as unstable). But, the aliphatic index of *RET* protein was high (82.25), which reveals that this protein may be stable for a wide range of temperature. The grand average of hydropathicity index was very low and slightly different between wild-type and mutated structures, which infer that these proteins could result in better and different interactions with, water.

The predicted models (wild-type and mutated) were flexibly docked with two ligands (ZD-6474 and ponatinib), where out of ten poses produced, the best ligand pose was selected based on top score and the target structure was chosen for further analysis. Docking results of ZD-6474 and wild-type structure indicated that amino acid residues (GLU 337, ASP 353, ARG 355, GLY 453, PHE 646, and LEU 1018) in the *RET* protein play an important role in maintaining a functional conformation and directly involved in ligand binding (Figure 5A), while in the C.G2901A (P.C634Y) mutation, amino acid residues (GLU 337, ASP 353, ARG 355, ALA 458, PHE 646, and LEU 1018) in the *RET* protein play This role (Figure 5B). In case of docking this ligand in the C.G2901T (P.C634F) mutated structure these amino acid residues were slightly changed (ASP 353, ARG 355, GLY 453, PHE 646, TYR 1015 and LEU 1018) (Figure 5C), hence, for C.G2251A (P.G691S) mutated *RET* protein the amino acid residues were ARG 355, TYR 461, VAL 642, SER 645, TYR 1015 and LEU 1018 (Figure 5D).

Besides, Docking results of ponatinib and wild-type structure indicated that amino acid residues (GLU 337, ARG 355, GLY 453, GLU 459, PHE 646, and LEU 1018) in the *RET* protein play an important role in maintaining a functional conformation and directly involved in ligand binding (Figure 6A), while in the C.G2901A (P.C634Y) mutation, amino acid residues (VAL 331, GLU 337, ARG 355, GLU 337, ARG 368, VAL 454, ALA 458, GLU 459, and PHE 646) in the *RET* protein play This role (Figure 6B). In case of docking this ligand in the C.G2901T (P.C634F) mutated structure these amino acid residues were GLU 337, ARG 355, GLU 337, ARG 368, VAL 454, ALA 458, GLU 459, and PHE 646 (Figure 6C), hence, for C.G2251A (P.G691S) mutated *RET* protein the amino

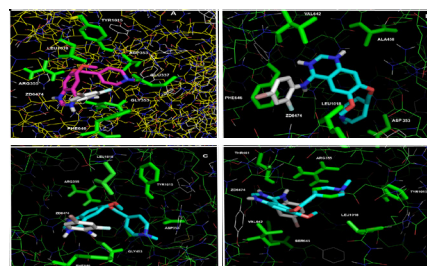


**Figure 5. The Predicted Binding Mode of the ZD-6474 Inhibitor (in Sticks Model) with the *RET* Binding Site Residues are Shown in Line Models. A) superposition of the predicted binding mode (in stick model) with the crystallographic conformation of the ZD-6474 inhibitor from the WT complex (default colors, stick model); B) C.G2901A (P.C634Y) *RET* mutant; C) C.G2901T (P.C634F) *RET* mutant; D) C.G2251A (P.G691S) *RET* mutant**

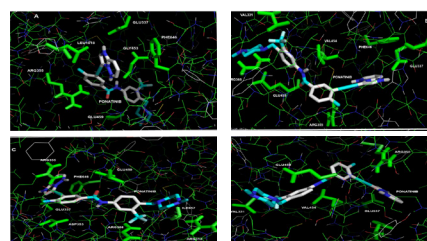


**Figure 6. The Predicted Binding Mode of the ponatinib Inhibitor (in Sticks Model) with the *RET* Binding Site Residues are Shown in Line Models. A) superposition of the predicted binding mode (in stick model) with the crystallographic conformation of the ponatinib inhibitor from the WT complex (default colors, stick model); B) C.G2901A (P.C634Y) *RET* mutant; C) C.G2901T (P.C634F) *RET* mutant; D) C.G2251A (P.G691S) *RET* mutant**

acid residues were VAL 331, GLU 337, ARG 355, GLU 337, ARG 368, VAL 454, ALA 458, GLU 459, and PHE 646 (Figure 6D).

Although the ZD-6474 and ponatinib inhibitors make hydrogen bonds with wild-type and mutated structures, the size of the side chain at this position is important in controlling access to the binding pocket. Indeed, simulations with the C.G2901A (P.C634Y) *RET* mutant suggest a more tightly bound conformation of the both inhibitors (Table 1). These changes may only partially improve the intermolecular inhibitor interactions. In contrast, C.G2251A (P.G691S) mutations may interfere with binding the inhibitor and render resistance to both inhibitors.

Indeed, C.G2901A (P.C634Y) and C.G2901T

(P.C634F) *RET* mutations, which have the oncogenic activity, may result in the largest destabilization effect on the inactive kinase structure (Table 2). In contrast, the transforming potential of *RET* mutations at G691 positions is known to be very small, so it may have stabilizing effect on the kinase structure (Table 2).

## Discussion

Mutations in the hot spot exons of the *RET* proto-oncogene and the disease phenotype-genotype have been well studied, allowing prediction of the clinical manifestations of specific mutations in MEN 2A (Eng et al., 1996). Here, we report the identification of a case of MEN 2A associated with C.G2901T (P.C634F), C.G2901A (P.C634Y) and G691F *RET* sequence alteration, as well as modeling the *RET* protein, assess the stability change due to mutations, and observing the effect of mutation on inhibitors binding.

Studies on white populations with hereditary MTC showed different *RET* proto-oncogene mutations in various populations and ethnic groups, for example, the largely main mutation in Spain and France was at codon 634 (Schuffenecker et al., 1998; Robledo et al., 2003). In Italy the highest and the lowest mutation rates of *RET* proto-oncogene mutation were belong to codons 804 and 634 in familial MTC, respectively, and in sporadic form was mutation at codon 918 (Pinna et al., 2007; Saggiorato et al., 2007). In Portugal and Czech Republic, the most common mutation was codon 918 for the sporadic form of MTC (Zedenius et al., 1994). In USA the most common mutation in this gene was at codon 634 in patients with hereditary MTC (Moura et al., 2009). In Iran and China also the highest genetic variation and mutation was reported at codon 634 (Zhou et al., 2007; Hedayati et al., 2011). Thus, it seems that mutation of codon 634 is the most common *RET* proto-oncogene mutation in MTC.

**Table 1. Structure and Final Docking Energy of Selected Inhibitors to Wild-Type and Mutated *RET* Protein**

Parameters		Wild type	MutC 634Y	MutC 634F	MutG 691F
ZD-6474	Binding affinity	-8.2	-8.3	-8.4	-8.3
	Final docking energy	-12.19	-12.31	-11.43	-11.61
Ponatinib	Binding affinity	-9.7	-9.7	-9.7	-9.7
	Final docking energy	-13.21	-14.37	-13.13	-12.88

Binding affinity, Sum of final intermolecular energy (kcal/mol); Final docking energy, Sum of final intermolecular energy and final internal energy of ligand (kcal/mol)

**Table 2. Structural Mapping of Cancer Mutations and Modeling Protein Stability Effects in the *RET* Proto-Oncogene. Protein Stability Differences between the Wild-Type and Mutants *RET* Using SDM, CUPSAT, FOLDx, and MUpro**

Model	$\Delta\Delta G$ (kcal/mol)				Stability change	Solvent accessibility		SDM The effect of mutation
	SDM	CUPSAT	FOLDx	MUpro		Mutated	Wild-type	
Mutated C634F	-1.85	-0.69	-1.9	-0.96	Destabilizing	8.5% (buried)	8.5% (buried)	Non-disease-associated Toombak dipping
Mutated C634Y	-2.87	-0.5	-0.01	-0.85	Highly destabilizing	8.4% (buried)	7.8% (buried)	Cause protein malfunction and disease
Mutated G691S	1.54	0.41	0.27	0.8	Stabilizing	106.5% (accessible)	101.6% (accessible)	Non-disease-associated

Codon 634 of *RET* proto-oncogene is coding for one of five cysteine residues of the extracellular part of the *RET* protein, and missense mutation at this codon is the one most frequently associated with MEN 2A syndrome (Mulligan et al., 1995). Specific nucleotide and amino acid exchanges at codon 634 leads in ligand-independent receptor dimerization and auto-phosphorylation, converting the mutated allele to a dominant transforming gene (Asai et al., 1995), and might have a direct impact on tumor aggressiveness in MEN 2A syndrome (Punales et al., 2003). Previously, it has been clearly suggested that C.G2251A (P.G691S) mutation of the *RET* is related to the early appearance of symptoms in MEN 2A patients; therefore, it is not oncogenic per se (Borrello et al., 2011), and may consider as a low penetrance gene or genetic modifier that associates with a small to moderate increased risk for developing a MTC (Robledo et al., 2003). Our results of mutation-based stability change in *RET*, showed C.G2901A (P.C634Y) and C.G2901T (P.C634F) mutations as destabilizing, hence C.G2251A (P.G691S) mutation as stabilizing factor. The possible reason is that Cysteine 634 is located at cysteine-rich region; while Glycine 691 is placed on transmembrane domain of *RET* protein.

Recently, Some researchers revealed that mutation-induced drug resistance may significantly impair the potency of the inhibitors in various cancers treatment, thus in silico and bioinformatics tools can provide powerful and efficient techniques in investigating drug resistance (Segbena et al., 2012; Brady et al., 2013; Wang et al., 2013). Although the *RET*-targeting agents ZD-6474 and ponatinib have improved the survival of patients with MTC, resistance to these targeted therapies is remaining as a major challenge (De Falco et al., 2013; Ton et al., 2013). Ponatinib is a tyrosine kinase inhibitor that is tested on *RET* oncogenic activity, in which the results showed that it is a useful inhibitor in a *RET* mutation-induced resistance via blunting mutant phosphorylation and rearranged *RET* onco-protein (De Falco et al., 2013). Our result was in consistency and showed better binding affinity and final docking energies for ponatinib compared to the ZD-6474.

Dixit et al. (2009) studied the impact of M918T in *RET* located on tyrosine kinase domain, dynamics, and stability using homology modeling, molecular dynamic and simulation procedures, as well as docked ZD-6474 and assessed the effect of this mutation on drug binding fashion. They showed that structural mapping of *RET* oncogenic mutations and the observed protein stability changes using in silico methods suggested that these mutations tend to have the greatest destabilization effect

on the *RET* protein structure (Dixit et al., 2009). Anders et al investigated the structural organization of the *RET* cadherin-like domain using in silico, mutagenesis, and binding studies. They claimed that cadherin-like domain of *RET*, which modeled by in silico methods represent valuable tools to guide future site-directed mutagenesis studies aimed at identifying residues involved in ligand binding and receptor activation (Anders et al., 2001).

In conclusion, the prevalence of *RET* proto-oncogene mutations is relatively high in Iranian patients with MTC, so that in these patients, genetic studies are necessary. In silico, and computer-aided molecular dynamic and simulations of the mutations in the *RET* proto-oncogene have allowed scientist to study the impact of these mutations in altering the protein structure, dynamics, and stability more efficiently. Also, simultaneous study of the cancer mutations using both in silico and medical genetic procedures, as well as study the onco-protein inhibitors binding fashion considering the mutation-induced drug resistance may help in better overcoming the chemotherapy resistances and designing innovative drug discovery in cancer research. The functional effect of a structurally important mutational hotspot in the *RET* proto-oncogene, shared by C.G2901T (P.C634F), C.G2901A (P.C634Y) and C.G2251A (P.G691S), has been interp *RET*ed by simulating the differential effect of these mutations. We have found that mechanistic basis of the activating *RET* cancer mutations may be driven by an appreciable free energy destabilization or stabilization depending on the mutated amino acid. The computed protein stability differences between the wild-type and cancer mutants may provide a molecular rationale of the observed phenomenon.

## References

- Anders J, Kjar S, Ibanez CF (2001). Molecular modeling of the extracellular domain of the *RET* receptor tyrosine kinase reveals multiple cadherin-like domains and a calcium-binding site. *J Biol Chem*, **276**, 35808-17.
- Asai N, Iwashita T, Matsuyama M, Takahashi M (1995). Mechanism of activation of the *RET* proto-oncogene by multiple endocrine neoplasia 2A mutations. *Mol Cell Biol* **15**, 1613-9.
- Borrello MG, Aiello A, Peissel B, et al (2011). Functional characterization of the MTC-associated germline *RET*-K666E mutation: evidence of oncogenic potential enhanced by the G691S polymorphism. *Endocr Relat Cancer*, **18**, 519-27.
- Bowie JU, Luthy R, Eisenberg D (1991). A method to identify protein sequences that fold into a known three-dimensional structure. *Science*, **253**, 164-70.
- Brady SW, Zhang J, Seok D, Wang H, Yu D (2014). Enhanced PI3K p110alpha signaling confers acquired lapatinib resistance that can be effectively reversed by a p110alpha-selective PI3K inhibitor. *Mol Cancer Ther*, **13**, 60-7
- Cheng J, Randall A, Baldi P (2006). Prediction of protein stability changes for single-site mutations using support vector machines. *Proteins*, **62**, 1125-32.
- Colovos C, Yeates TO (1993). Verification of protein structures: patterns of nonbonded atomic interactions. *Protein Sci*, **2**, 1511-9.
- Cosconati S, Forli S, Perryman AL, Harris R, Goodsell DS, Olson AJ (2010). Virtual Screening with AutoDock: Theory and Practice. *Expert Opin Drug Discov*, **5**, 597-60.
- De Falco V, Buonocore P, Muthu M, Torregrossa L, Basolo F, Billaud M, et al (2013). Ponatinib (AP24534) is a novel potent inhibitor of oncogenic *RET* mutants associated with thyroid cancer. *J Clin Endocrinol Metab*, **98**, 811-9.
- Dixit A, Torkamani A, Schork NJ, Verkhivker G (2009). Computational modeling of structurally conserved cancer mutations in the *RET* and *MET* kinases: the impact on protein structure, dynamics, and stability. *Biophys J*, **96**, 858-74.
- Eng C, Clayton D, Schuffenecker I, et al (1996). The relationship between specific *RET* proto-oncogene mutations and disease phenotype in multiple endocrine neoplasia type 2. International *RET* mutation consortium analysis. *JAMA*, **276**, 1575-9.
- Hedayati M, Nabipour I, Rezaei-Ghaleh N, Azizi F (2006). Germline *RET* mutations in exons 10 and 11: an Iranian survey of 57 medullary thyroid carcinoma cases. *Med J Malaysia*, **61**, 564-9.
- Hedayati M, Zarif Yeganeh M, Sheikhol Eslami S, et al (2011). Predominant *RET* germline mutations in exons 10, 11, and 16 in Iranian patients with hereditary medullary thyroid carcinoma. *J Thyroid Res*, **2011**: 264248.
- Kaplan W, Littlejohn TG (2001). Swiss-PDB Viewer (Deep View). *Brief Bioinform*, **2**, 195-7.
- Kollman PA, Massova I, Reyes C, et al (2000). Calculating structures and free energies of complex molecules: combining molecular mechanics and continuum models. *Acc Chem Res*, **33**, 89-97.
- Kouvaraki MA, Shapiro SE, Perrier ND, et al (2005). *RET* proto-oncogene: a review and update of genotype-phenotype correlations in hereditary medullary thyroid cancer and associated endocrine tumors. *Thyroid*, **15**, 531-544.
- Laskowski RA, Rullmannn JA, MacArthur MW, Kaptein R, Thornton JM (1996). AQUA and PROCHECK-NMR: programs for checking the quality of protein structures solved by NMR. *J Biomol NMR*, **4**, 477-86.
- Matias-Guiu X, De Lellis R (2013). medullary thyroid carcinoma: a 25-year perspective. *Endocr Pathol*. [Epub ahead of print].
- Moura MM, Cavaco BM, Pinto AE, Domingues R, Santos JR, Cid MO, et al (2009). Correlation of *RET* somatic mutations with clinicopathological features in sporadic medullary thyroid carcinomas. *Br J Cancer*, **100**, 1777-83.
- Mulligan LM, Marsh DJ, Robinson BG, et al (1995). Genotype-phenotype correlation in multiple endocrine neoplasia type 2: report of the International *RET* Mutation Consortium. *J Intern Med*, **238**, 343-6.
- Nikiforova MN, Nikiforov YE (2008). Molecular genetics of thyroid cancer: implications for diagnosis, treatment and prognosis. *Expert Rev Mol Diagn*, **8**, 83-95.
- Othman NH, Omar E, Naing NN (2009). Spectrum of thyroid lesions in hospital Universiti Sains Malaysia over 11years and a review of thyroid cancers in Malaysia. *Asian Pac J Cancer Prev*, **10**, 87-90.
- Parthiban V, Gromiha MM, Schomburg D (2006). CUPSAT: prediction of protein stability upon point mutations. *Nucleic Acids Res*, **34**, 239-42.
- Pinna G, Orgiana G, Riola A, Ghiani M, Lai ML, Carcassi C, et al (2007). *RET* proto-oncogene in Sardinia: V804M is the most frequent mutation and may be associated with FMTC/MEN-2A phenotype. *Thyroid*, **17**, 101-4.
- Pronk S, Pall S, Schulz R, et al (2013). GROMACS 4.5: a high-throughput and highly parallel open source molecular simulation toolkit. *Bioinformatics*, **29**, 845-54.
- Punales MK, Graf H, Gross JL, Maia AL (2003). *RET* codon 634 mutations in multiple endocrine neoplasia type 2: variable

- clinical features and clinical outcome. *J Clin Endocrinol Metab*, **88**, 2644-9.
- Punales MK, Rocha AP, Gross JL, Maia AL (2004). [Medullary thyroid carcinoma: clinical and oncological features and treatment]. *Arq Bras Endocrinol Metabol*, **48**, 137-46.
- Robledo M, Gil L, Pollan M, et al (2003). Polymorphisms G691S/S904S of *RET* as genetic modifiers of MEN 2A. *Cancer Res*, **63**, 1814-7.
- Saggiorato E, Rapa I, Garino F, et al (2007). Absence of *RET* gene point mutations in sporadic thyroid C-cell hyperplasia. *J Mol Diagn*, **9**, 214-9.
- Sali A, Blundell TL (1993). Comparative protein modelling by satisfaction of spatial restraints. *J Mol Biol*, **234**, 779-815.
- Santoro M, Carlomagno F, Melillo RM, Fusco A (2004). Dysfunction of the *RET* receptor in human cancer. *Cell Mol Life Sci*, **61**, 2954-64.
- Schuffenecker I, Virally-Monod M, Brohet R, et al (1998). Risk and penetrance of primary hyperparathyroidism in multiple endocrine neoplasia type 2A families with mutations at codon 634 of the *RET* proto-oncogene. Groupe D'etude des tumeurs a calcitonine. *J Clin Endocrinol Metab*, **83**, 487-91.
- Schymkowitz J, Borg J, Stricher F, et al (2005). The FOLDX web server: an online force field. *Nucleic Acids Res*, **33** 382-8.
- Segbena AY, Kueviakoe IM, Agbetiafa K, et al (2012). Chronic myeloid leukemia and imatinib: experience at the lome campus teaching hospital (Togo). *Med Sante Trop*, **22**, 307-11.
- Srinivasan J, Miller J, Kollman PA, Case DA (1998). Continuum solvent studies of the stability of RNA hairpin loops and helices. *J Biomol Struct Dyn*, **16**, 671-82.
- Ton GN, Banaszynski ME, Kolesar JM (2013). Vandetanib: a novel targeted therapy for the treatment of metastatic or locally advanced medullary thyroid cancer. *Am J Health Syst Pharm*, **70**, 849-55.
- Verkhivker GM, Bouzida D, Gehlhaar DK, et al (2003). Computational detection of the binding-site hot spot at the remodeled human growth hormone-receptor interface. *Proteins*, **53**, 201-19.
- Verkhivker GM, Bouzida D, Gehlhaar DK, et al (2002). Monte Carlo simulations of the peptide recognition at the consensus binding site of the constant fragment of human immunoglobulin G: the energy landscape analysis of a hot spot at the intermolecular interface. *Proteins*, **48**, 539-57.
- Wang DD, Zhou W, Yan H, Wong M, Lee V (2013). Personalized prediction of EGFR mutation-induced drug resistance in lung cancer. *Sci Rep*, **3**, 2855.
- Wang J, Wolf RM, Caldwell JW, Kollman PA, Case DA (2004). Development and testing of a general amber force field. *J Comput Chem*, **25**, 1157-74.
- Wiederstein M, Sippl MJ (2007). ProSA-web: interactive web service for the recognition of errors in three-dimensional structures of proteins. *Nucleic Acids Res*, **35**, 407-10.
- Worth CL, Preissner R, Blundell TL (2011). SDM-a server for predicting effects of mutations on protein stability and malfunction. *Nucleic Acids Res*, **39**, 215-22.
- Zedenius J, Wallin G, Hamberger B, et al (1994). Somatic and MEN 2A de novo mutations identified in the *RET* proto-oncogene by screening of sporadic MTC:s. *Hum Mol Genet*, **3**, 1259-62.
- Zhang Y (2008). I-TASSER server for protein 3D structure prediction. *BMC Bioinformatics*, **9** 40.
- Zhou Y, Zhao Y, Cui B, et al (2007). *RET* proto-oncogene mutations are restricted to codons 634 and 918 in mainland Chinese families with MEN2A and MEN2B. *Clin Endocrinol*, **67**, 570-6.